Aalborg Universitet

AALBORG UNIVERSITY
DENMARK

Embedment Effects on Vertical Bearing Capacity of Offshore Bucket Foundations on Cohesionless Soil

Barari, Amin; Ibsen, Lars Bo; Ghalesari, Abbasali Taghavi; Larsen, Kim Andre

Published in:
International Journal of Geomechanics

DOI (link to publication from Publisher):
10.1061/(ASCE)GM.1943-5622.0000782

Publication date:
2017

Document Version
Accepted author manuscript, peer reviewed version

Link to publication from Aalborg University

Citation for published version (APA):
Barari, A., Ibsen, L. B., Ghalesari, A. T., & Larsen, K. A. (2017). Embedment Effects on Vertical Bearing Capacity of Offshore Bucket Foundations on Cohesionless Soil. *International Journal of Geomechanics*, *17*(4). https://doi.org/10.1061/(ASCE)GM.1943-5622.0000782

General rights
Copyright and moral rights for the publications made accessible in the public portal are retained by the authors and/or other copyright owners and it is a condition of accessing publications that users recognise and abide by the legal requirements associated with these rights.

- Users may download and print one copy of any publication from the public portal for the purpose of private study or research.
- You may not further distribute the material or use it for any profit-making activity or commercial gain
- You may freely distribute the URL identifying the publication in the public portal -

Take down policy
If you believe that this document breaches copyright please contact us at vbn@aub.aau.dk providing details, and we will remove access to the work immediately and investigate your claim.

Embedment Effects on Vertical Bearing Capacity of Offshore Bucket Foundations on Cohesionless Soil

A. Barari, A.M.ASCE[1]; L. B. Ibsen, M.ASCE[2]; A. Taghavi Ghalesari[3]; and K. A. Larsen[4]

Abstract: This paper presents the results from a series of physical modeling and three-dimensional finite-element (FE) analyses in which the authors examined the uniaxial vertical capacity of suction caissons for offshore wind turbines. The experiments were carried out in quartz sand and involved monotonic application of vertical load. It was found that the drained capacity of suction caissons is dependent on embedment ratio. In contrast, predictions from conventional semiempirical depth factors were found to somewhat underestimate when applied to rough foundations. On the basis of the tests and FE analyses, new expressions for the depth factor of shallow foundations were validated for embedment ratios (aspect ratios) up to unity, calibrating the fitting parameters by using data from a range of soil profiles. **DOI: 10.1061/(ASCE)GM.1943-5622.0000782.** *© 2016 American Society of Civil Engineers.*

Author keywords: Vertical bearing capacity; Reduced friction angle; Bucket foundation; Solid foundation; Aalborg University Sand No. 1.

Downloaded from ascelibrary.org by Amin Barari on 09/30/16. Copyright ASCE. For personal use only; all rights reserved.

Introduction

With the current demand for green energy technologies, there are strong industrial and economical scenarios for developing the offshore wind energy sectors in which rate of expansion overtakes the even levels observed during the heyday of the offshore oil and gas industry. For example, a detailed program including three rounds was established in the U.K. offshore wind energy sector by submitting proposals for a number of wind farms in the coastal waters surrounding the U.K. For such developments, alternative low-cost and low-risk platforms must be rearranged (e.g., four-legged jackets, tripods, floating systems, and suction caissons) (Bhattacharya et al. 2013; Barari and Ibsen 2012, 2014).

The majority of 485 suction anchors reported by Andersen et al. (2005) were installed for anchoring floaters in clay by the year 2004. Tjelta (1995) reported exemplar shallow foundations at Draupner E and Sleipner T sites in the North Sea (Tjelta 1995).

Although the findings of previous research carried out on suction caissons in oil and gas platforms are significant, they are not consistent with those of offshore renewable energy platforms. The nondimensional framework to provide information for understanding the vertical load on these relatively novel structures [$V/(\gamma' d^3)$, where γ' is unit buoyant weight and d is skirt length) lies over a range of 0.5–0.8. In oil and gas facilities, it is well documented that a suction caisson is exposed to a nondimensional vertical load of 3.5. General loading is particularly relevant in the design of shallow foundations for offshore structures, because wind, wave, and current forces provide substantial lateral load components of magnitudes that are not commonly encountered onshore. Therefore, establishment of new design drivers under these circumstances is recommended.

Brief Summary of Existing Literature

The performance of offshore shallow foundations has been a topic of research throughout the last decades. Plasticity-based analyses initially suggested by Roscoe and Schofield (1956) may be constructed in terms of the force resultants acting on the footings and the corresponding displacements. This approach has been further developed by others, and generalizes the concept of vertical bearing capacity proposed by Terzaghi (1943) to take the load eccentricity effect into account (Tahmasebi poor et al. 2015). Experimental studies have provided the data necessary to establish the combined loading interaction diagrams on sands (Nova and Montrasio 1991; Butterfield and Gottardi 1994; Cassidy 2007; Gottardi and Butterfield 1993, 1995; Byrne and Houlsby 2001; Larsen et al. 2013). The programs of Martin (1994), Byrne and Houslby (2001), and Ibsen et al. (2014a, b, 2015) also resulted in complete plasticity models that describe the behavior of circular footings in terms of combined forces (V, H, M) and associated degrees of freedom.

The strain-hardening models have major components, including yield envelope in terms of three-dimensional (3D) loading space (V-H-M), hardening rule, and flow rule. The size of the empirical expression for yield surface is controlled by the vertical capacity, defined by V_0. The terminology of hardening law, which is defined by variation of yield surface size, was initially assumed to be a function of plastic vertical displacement [$V = f(w_p)$].

A typical three-dimensional yield envelop in (V, H, M) space is shown in Fig. 1 and is described by a closed-form expression in terms of normalized loads given by Gottardi et al. (1999)

$$f = \left(\frac{m_n}{m_0}\right)^2 + \left(\frac{h_n}{h_0}\right)^2 - 2a\left(\frac{h_n m_n}{h_0 m_0}\right) - 1 \tag{1}$$

where

[1]Postdoctoral Researcher, Dept. of Civil and Environmental Engineering, Virginia Tech, Blacksburg, VA 24061 (corresponding author). E-mail: abarari@vt.edu; amin78404@yahoo.com

[2]Professor, Dept. of Civil Engineering, Aalborg Univ., Sofiendalsvej 9200 Aalborg, Denmark. E-mail: lbi@civil.aau.dk

[3]Researcher in Civil Engineering, Babol Univ. of Technology, Babol 47148-71167, Mazandaran, Iran.

[4]Researcher in Civil Engineering, Cowi A/S, 9000 Aalborg, Denmark.

Note. This manuscript was submitted on July 2, 2015; approved on July 5, 2016; published online on September 30, 2016. Discussion period open until March 1, 2017; separate discussions must be submitted for individual papers. This paper is part of the ***International Journal of Geomechanics***, © ASCE, ISSN 1532-3641.

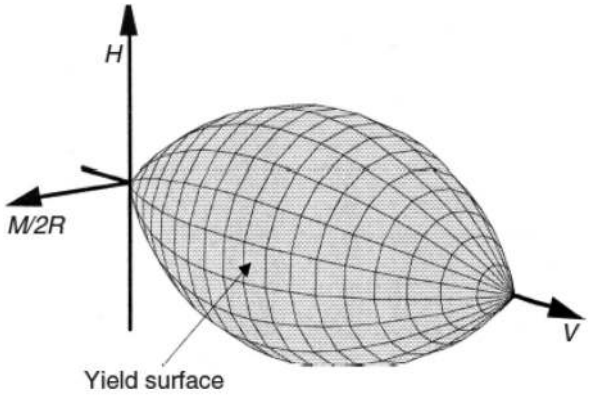

Fig. 1. Schematic view of yield surface for shallow foundations

$$m_n = \frac{M/DV_0}{4v(1-v)}$$
$$h_n = \frac{H/V_0}{4v(1-v)}$$
$$v = \frac{V}{V_0} \tag{2}$$

where a = failure surface parameter; and V_0 = apex of the surface formulating its size and is determined by the hardening law. In other words, if the yield locus curve is normalized in terms of V/V_0, it is necessary to obtain the V_0 for a foundation to obtain the size of the yield locus. The subscript 0 is used to emphasize the work-hardening behavior of the sand–foundation interaction.

An empirical hardening expression that fits the experimental data for circular footings on dense sand is (Gottardi et al. 1999)

$$V = \frac{k_p w_p}{1 + \left(\frac{k_p w_{pm}}{V_m} - 2\right)\left(\frac{w_p}{w_{pm}}\right) + \left(\frac{w_p}{w_{pm}}\right)^2} \tag{3}$$

where k_p = initial plastic stiffness; V_m = maximum vertical load; and w_{pm} = value of w_p at the maximum load.

Purpose and Scope of Paper

Although the bearing capacity of shallow foundations is a long researched topic, for the case of suction caissons, the capacity is difficult to calculate accurately. This is because of the (1) clear difference between offshore and onshore shallow foundation systems and loading conditions, whereas the industry-recommended practice for offshore shallow foundation design was developed from onshore design codes [for example, the selection of individual European country guidelines (Sieffert and Bay-Gress 2000); (2) existence of embedment; and (3) difficulties in finding appropriate bearing capacity factors (Ibsen et al. 2012; Tahmasebi poor et al. 2015).

The combination of the aforementioned difficulties is investigated in this paper predominantly using small-scale model tests and finite-element (FE) analyses. A consistent formulation for vertical capacity of suction caissons for offshore wind turbines and, therefore, size of yield surface envelope was established herein.

Suction Caissons for Offshore Wind Turbines

Suction caissons can also be used to increase the moment fixity and can be an attractive solution for offshore wind turbines, as the bucket foundation installed in Frederikshavn has shown (Ibsen 2008). There

Fig. 2. Prototype of bucket foundations (reprinted from Barari 2012, with permission)

Fig. 3. Bucket foundation for the Vestas 3-MW wind turbine in Frederikshavn (reprinted from Barari 2012, with permission)

are two stages for the suction caisson installation. First, the caisson penetrates soil by self-weight to a certain depth, during which a sealed chamber is formed in the caisson. Then, water is pumped out from the sealed chamber in the caisson to create pressure difference. The caisson is driven into the soil further by the pressure difference.

The steel bucket consists of a vertical steel skirt extending down from a horizontal base resting on the soil surface. A prototype of the bucket foundation is shown in Fig. 2.

In addition to the limitations in suction, the risk of buckling in the skirt during penetration must be considered during design of the bucket foundation. Experience from installation tests with large-scale buckets has shown that, if the critical suction is exceeded, the situation can be stabilized by adding soil to the seabed in the area of the piping hole outside the bucket foundation. After dissipation of the pore pressure in the soil, the installation procedure can be continued. Several studies have examined the critical gradient and penetration resistance of suction-installed bucket foundations in sand (Feld 2001; Houlsby et al. 2005; Houlsby and Byrne 2005).

In November 2002, the first bucket foundation for a fully operational wind turbine was installed in Frederikshavn, a city in the northern part of Jutland, Denmark (Ibsen et al. 2005) (Fig. 3). When installed, the V90-3.0 MW wind turbine (Vestas, Aarhus, Denmark) was the largest wind turbine in Denmark, with a total height of

Downloaded from ascelibrary.org by Amin Barari on 09/30/16. Copyright ASCE. For personal use only; all rights reserved.

125 m. The bucket foundation had a diameter of 12 m, skirt length of 6 m, and total weight of 135 t. Installation of the bucket foundation was carried out by the geotechnical department of Aalborg University (Ibsen et al. 2005).

Vertical Capacity of Suction Caissons for Offshore Wind Turbines: Existing Literature

Byrne et al. (2003) investigated the vertical bearing capacity of circular surface footings and bucket foundations in dry sand, with D_r = 88% and embedment ratios of the bucket foundation varying from 0 to 2. Their results are shown as the upper theoretical (gray) line in Fig. 4. The lower theoretical line represents the penetration resistance during installation reported by Houlsby and Byrne (2005) (and verified by Villabolos et al. 2005), which was calculated with the general bearing capacity formula for a strip foundation with plane strain bearing capacity factors. The Houlsby and Byrne (2005) method takes into account the enhanced stresses around the skirt and at the tip. Using the bearing capacity factors recommended in Eq. (4) and a friction angle of 37.6°, the present study obtained a new fit for the peak capacity, which captured the measured peak capacities well (Fig. 4)

$$N_\gamma = c_1 \cdot [(N_q - 1)\cos\phi]^{c_2}$$
$$N_q = c_3 \cdot e^{c_4 \cdot \pi \cdot \tan\phi} \tan^2\left(45 + \frac{\phi}{2}\right) \quad (4)$$

where the c_i values are given in Table 1. The values of the bearing capacity factors given by Eq. (4) are shown in Figs. 5 and 6.

Experimental Procedures

The test program involved installations of instrumented model caissons, including diameters (D) of 50, 100, and 200 mm and embedment ratios (d/D) of 0, 0.25, 0.5, 0.75, and 1. The loading tests were carried out on Aalborg University dense-saturated sand in a specially designed test box, and have evolved over subsequent parts of the capacity assessment (Part I, Part II, and Part III). The main details of the experimental setup are described by Ibsen et al. (2014a, b). Aalborg University Sand No. 1 primarily consists of quartz, but also contains feldspar and biotite. This sand has been widely used in the literature (Ibsen et al. 1995). All of the tests were performed in a Danish triaxial apparatus in the geotechnical laboratory at Aalborg University. The tests were all drained and performed on samples with a height/diameter ratio of 1 and with lubricated ends, according to Danish traditions. Sieve tests were utilized to investigate the distribution of the grains. The results revealed a mean grain size ($d50$) of 0.14 mm, coefficient of uniformity (U) of $d60/d10$ = 1.78, grain density (d_s) of 2.64, maximum void ratio (e_{max}) of 0.858, and minimum void ratio (e_{min}) of 0.549.

Experimental Results

Although there are a number of potential sources of discrepancy between results of laboratory tests and field performance, the dilatancy exhibited by the cohesionless soils at low stress levels in model tests may be a predominant factor. As a result, the higher peak friction angle pertaining to the soil in the model tests rather than soil with the same relative density present in the field could

Table 1. Coefficients in Eq. (4) for Bearing Capacity Factors

	Circular foundation		Strip foundation	
Coefficient	Smooth	Rough	Smooth	Rough
c_1	0.1	0.16	0.12	0.25
c_2	1.33	1.33	1.51	1.5
c_3	0.715	0.8	1	1
c_4	1.42	1.5	1	1

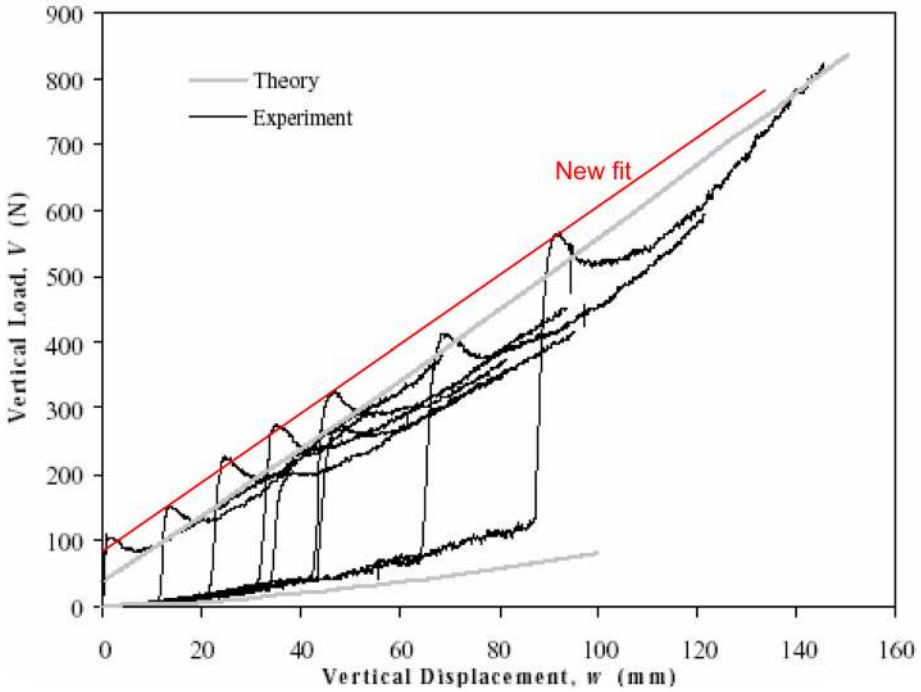

Fig. 4. Vertical load–displacement response from bearing capacity tests (data from Byrne et al. 2003)

Downloaded from ascelibrary.org by Amin Barari on 09/30/16. Copyright ASCE. For personal use only; all rights reserved.

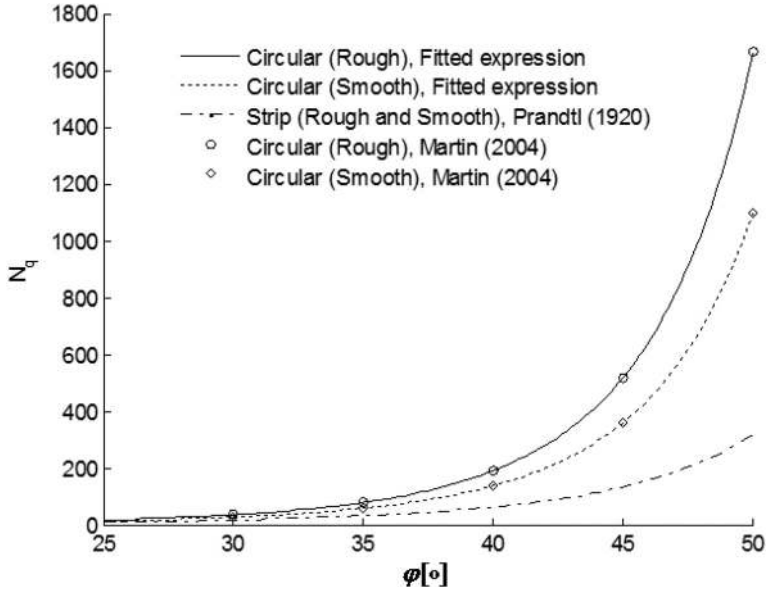

Fig. 5. Bearing capacity factor (N_q) for circular and strip foundations with smooth or rough bases

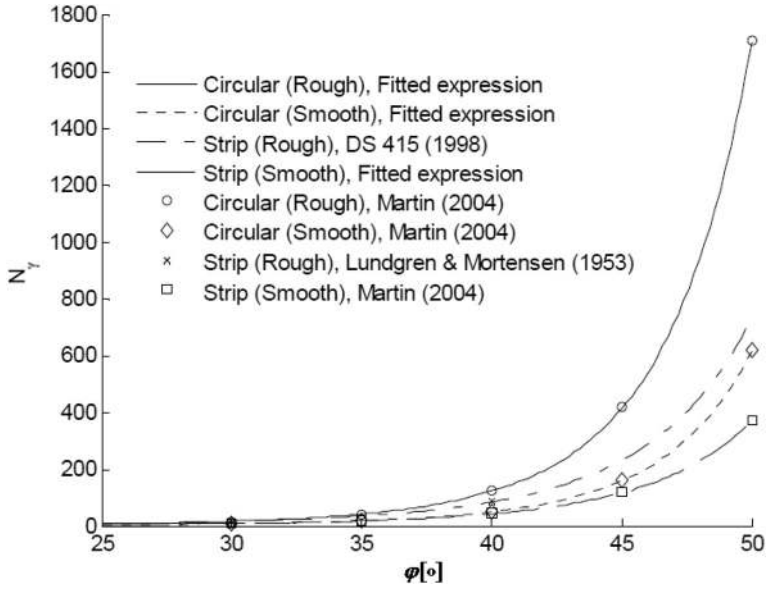

Fig. 6. Bearing capacity factor (N_γ) for circular and strip foundations with smooth or rough bases

affect the ultimate limit state of the soil-foundation system (Guo and Qin 2010; LeBlanc et al. 2010).

Accordingly, Ibsen et al. (2012) found a new theoretical relationship of the bearing capacity introducing the reduced friction angle for the analysis of the small-scale laboratory results. The reduced friction angle is determined herein by back-analysis of the results of bearing capacity tests for bucket foundations and the general bearing capacity formula as

$$V_{\text{peak}} = \gamma \frac{D}{2} N_\gamma \left(\frac{\pi D^2}{4}\right) + q N_q \left(\frac{\pi D^2}{4}\right) \tag{5}$$

where γ = unit soil weight; and q = overburden pressure estimated herein by $q = w \times \gamma$ (i.e., w = vertical settlement upon failure).

The new framework utilizing reduced friction angle does not account for the influence of overburden pressure induced by vertical settlements, other than parameters in the second term in Eq. (5) not contributing to the corrected vertical capacities.

The reduced friction angles for associated flow calculated from the measured capacities are shown in Fig. 7. These angles ranged from approximately 40° to 44°. Fig. 7 suggests that a linear relationship exists between the reduced friction angle and relative density for skirted foundations [Eq. (6)].

Hence, measured capacities from the vertical bearing capacity tests were successfully compared with the theoretical capacity values to be obtained using Eq. (6) with a friction angle of 42°, ignoring the contribution from the skirt friction

$$\varphi_d = 0.214 D_r + 22.86 \tag{6}$$

Results from the performed bearing capacity tests as a function of the embedment ratio (d/D) are shown in Figs. 8–10. The curve

Downloaded from ascelibrary.org by Amin Barari on 09/30/16. Copyright ASCE. For personal use only; all rights reserved.

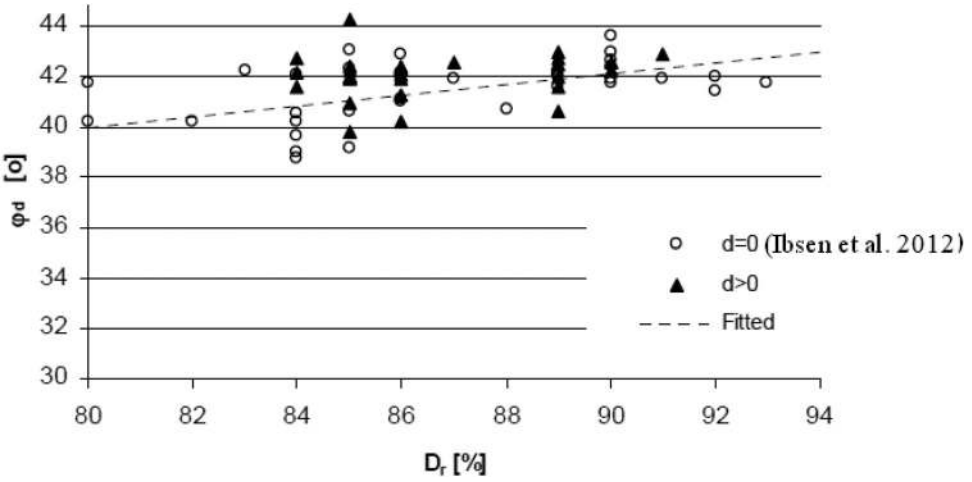

Fig. 7. ϕd calculated from V_{peak} and V_0 experiments

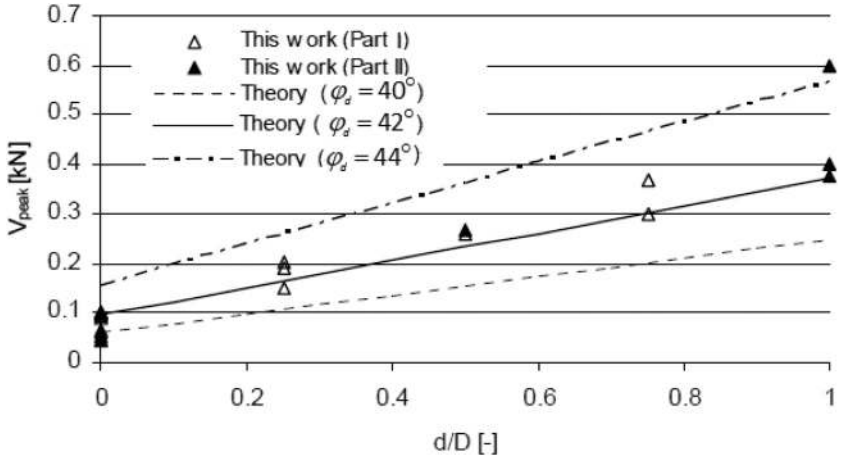

Fig. 8. Results from bearing capacity tests on buckets with $D = 50$ mm, corrected for deformations

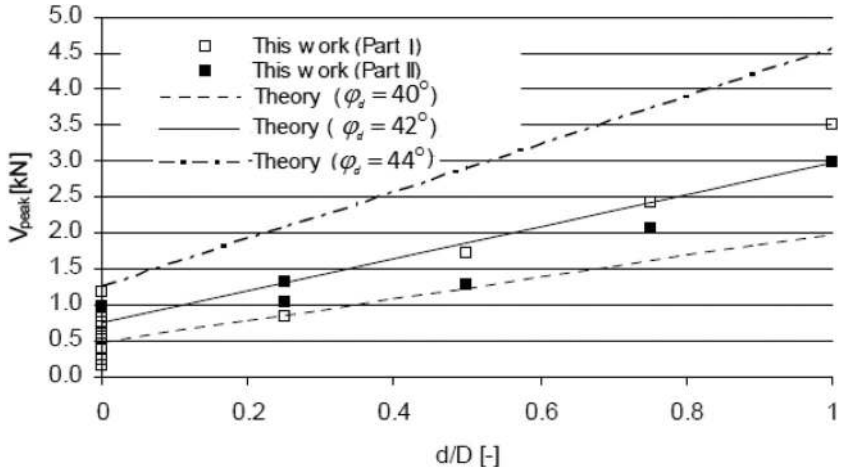

Fig. 9. Results from bearing capacity tests on buckets with D = 100 mm, corrected for deformations

fits were recommended for friction angles of 40°, 42°, and 44°. The theoretical bearing capacity agreed well with the measured capacities. Given the different soil profiles among the tests, the failure data are closely predicted by a reduced triaxial friction angle of 42°.

The results from the tests, which were corrected for the deformations at failure, are shown in Fig. 11. The normalized bearing capacities supported a linear relationship determined theoretically from the bearing capacity formula. Use of a mean friction angle of 42° yielded the following relationship:

Downloaded from ascelibrary.org by Amin Barari on 09/30/16. Copyright ASCE. For personal use only; all rights reserved.

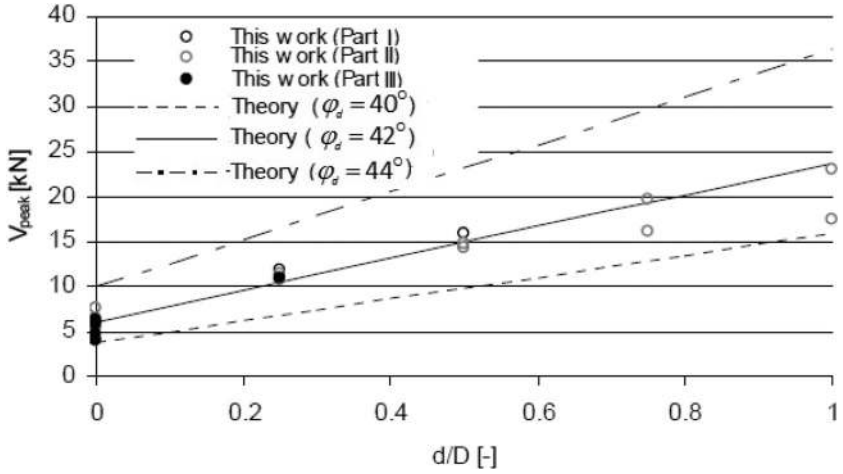

Fig. 10. Results from bearing capacity tests on buckets with $D = 200$ mm, corrected for deformations

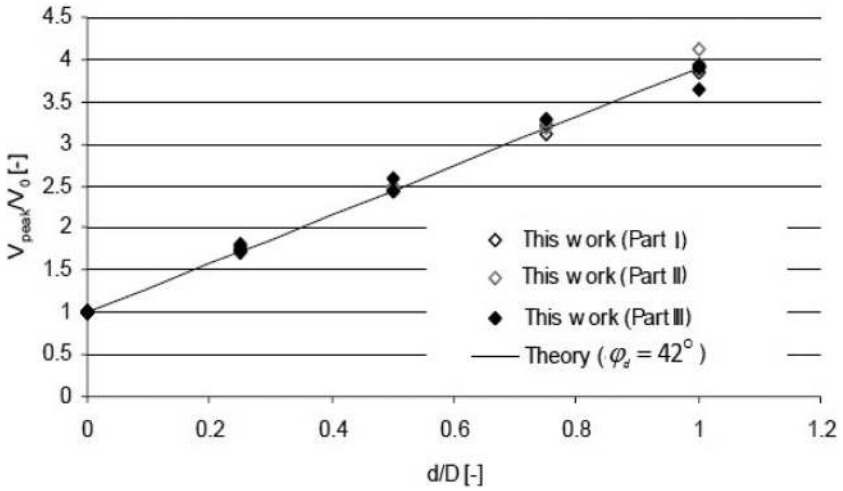

Fig. 11. Corrected vertical bearing capacity of bucket foundations normalized with the corresponding V_0 values

$$\frac{V_{\text{peak}}}{V_0} = 1 + 2.9\frac{d}{D} \tag{7}$$

The stress situation in the soil surrounding the foundation is unknown, but a mean value of the minor stress at failure can be estimated from Fig. 12. The reduced friction angle values shown in Fig. 12 were calculated from the triaxial-measured friction and dilation angles defined as

$$\tan \varphi_d = \frac{\sin \varphi \cos \psi}{1 - \sin \varphi \sin \psi} \tag{8}$$

The sand in the test box was deposited with a void ratio of approximately 0.61. This scenario corresponds to a mean value of the minor principal stress of approximately 15 kPa at failure for a reduced friction angle of $\varphi_d = 42°$. From the experiments, the corresponding triaxial and dilation angles at this stress level were $\varphi_{tr} = 47.5$ and $\psi = 17.5°$, respectively, for a void ratio of 0.61.

FE Model

The aforementioned results were verified in a 3D FE analysis using *PLAXIS 3D*. The capacity of a range of solid embedded and caisson foundations with a diameter of $D = 10$ m and a range of skirt lengths that penetrate to a depth d was investigated. By modeling the caisson as an embedded footing, it is implicitly assumed that there are no internal deformation mechanisms. Nine different meshes were required so that the precise configurations were modeled correctly. The suction caisson was modeled to be *wished in place* (i.e., ignoring the footing installation process).

Meshes, Geometry, and Material Parameters

A typical FE mesh discretization is shown in Fig. 13. The mesh comprises wedge continuum elements, and shallow foundations with embedment ratios (d/D) were considered. Each mesh comprised approximately 2,500 elements, including the aboveground structure.

An idealized homogeneous soil for a range of soil profiles was considered. The soil was modeled as a Mohr-Coulomb material (Table 2), and the foundation was modeled as an almost rigid element. The soil that was fully submerged was assumed to have a solid unit weight of 26.19 kN/m^3. Each analysis involved the initial application of gravity, including the tower and bucket in position prior to application of the vertical load. The c' component of the

Downloaded from ascelibrary.org by Amin Barari on 09/30/16. Copyright ASCE. For personal use only; all rights reserved.

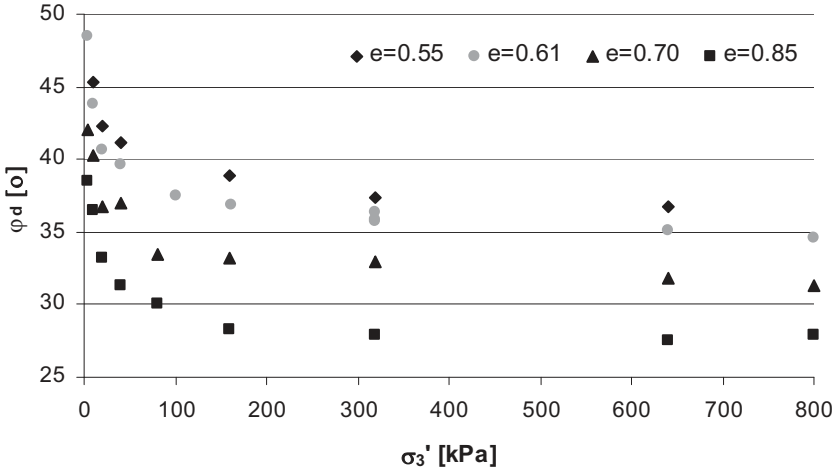

Fig. 12. Reduced friction angle derived from triaxial tests

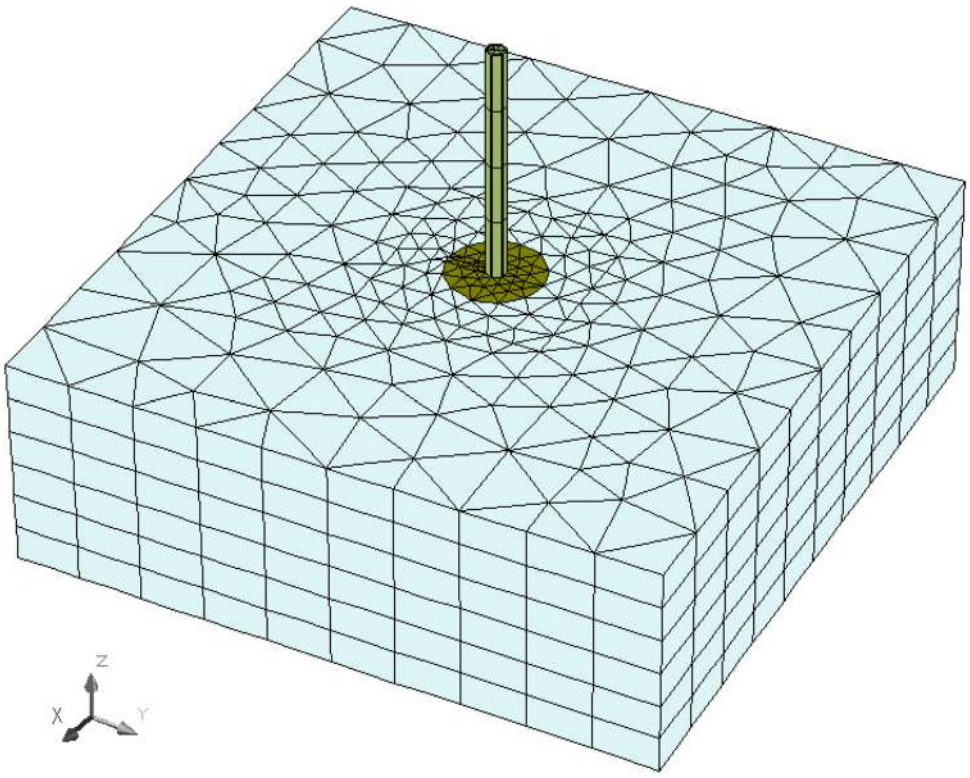

Fig. 13. Typical mesh discretization

strength was also taken as zero, and hence no tension was allowed in soil or between the foundation and soil.

The stress dependency of the oedometric stiffness modulus with the following formulation is incorporated into numerical models to account for the nonlinear soil behavior (Ohde 1939)

$$E = \kappa \sigma_{at} \left(\frac{\sigma_m}{\sigma_{at}} \right)^{\lambda} \tag{9}$$

where $\sigma_{at} = 100\,\mathrm{kN/m^2}$; and σ_m = current mean principal stress in the soil element.

The coefficient κ determines the soil stiffness at the reference stress state, and the parameter λ controls the stress dependency of the soil stiffness (EAU 2004).

The interface elements between the foundation and the soil were defined with the contact friction angle (δ) (i.e., two-thirds of the internal friction angle), preventing formation of gapping in foundation–soil contact. The relationship between shear and normal stresses transferred through the foundation and soil interface is governed by a modified Coulomb's friction theory (Jeong et al. 2004). A drained Poisson's ratio (ν') of 0.45 was also adopted.

Comparison of Solutions

Qualitatively, the analyses in Fig. 14 showed that the embedded foundations have a significantly higher capacity than the equivalent

Downloaded from ascelibrary.org by Amin Barari on 09/30/16. Copyright ASCE. For personal use only; all rights reserved.

surface ones. This is due to increasing the skin friction adjacent to the skirt area. This difference is consistently greater for higher D_r.

Accompanying deformation mechanisms highlighted the mechanistic reasons for almost similar response between the foundation types where the external wedges were extended into the soil zones above the level of footings base. In other words, the soil trapped within the skirts appears to displace as a rigid body, which explains the negligible difference in failure loads (Fig. 15).

Given the nature of deformation mechanisms, the skirted foundation capacities are slightly lower than for solid foundations with the proportional largest difference compared with the shallowest embedment (Fig. 14). Despite the salient changes in developing mechanisms between the shallower foundations, the difference in overall foundation capacity between the bucket and solid foundations with d/D = 1 and 0.25 increases from 7.6 to 18.4% for the dense soil models, respectively.

Previous work to solely obtain the bearing capacity from vertical loading (V_0) for a range of soil strength profiles and embedment ratios (d/D) (Davis and Booker 1973; Houlsby and Wroth 1983; Tani and Craig 1995) has relied mainly on either lower- or upper-bound plasticity analyses of shallow footings in undrained soil.

In Fig. 16, the FE results (Fig. 14) are compared with the existing solutions in the literature. It is convenient to present solutions for bearing capacity of embedded footings in terms of the depth ratio.

The tangent intersection method was used to determine the limit states (Mansur and Kaufman 1956).

Fig. 16 outlines the variation of predicted vertical bearing capacity factors [$V_{(d/D)} = d_{cV} V_{(d/D=0)}$]. Interestingly, despite diversity of the material models used, close agreement between calculations and measurements was achieved.

Plasticity solutions in terms of Hill- and Prandtl-type mechanisms for strip footing (Prandtl 1920) have been presented by Bransby and Randolph (1999) and are shown in Fig. 16. Formally, these solutions are upper bound.

Arguably, for suction caissons on dense deposits, it is also of interest to compare the ultimate depth factor (d_{cV}) computed in the FE analyses with a commonly used expression of Byrne and Houlsby (1999), who suggest taking the values of the bearing capacity factors given by Bolton and Lau (1993), which were previously found to be incorrect for foundations with a rough base. Accordingly, these factors are not applicable to offshore bucket foundations, which are assumed to be rough to prevent detachment between the

Table 2. Soil Properties (Data from Popescu and Prevost 1993)

Parameter	Loose sand ($D_r = 40\%$)	Medium sand ($D_r = 55\%$)	Dense sand ($D_r = 80\%$)
Mass density solid (kN/m^3)	26.19	26.19	26.19
Friction angle [ϕ (°)]	33	34.2	39.5
Oedometric stiffness parameter (κ)	400	500	600
Oedometric stiffness parameter (λ)	0.65	0.6	0.55
Poisson's ratio (ν)	0.45	0.45	0.45
Porosity	0.424	0.406	0.373

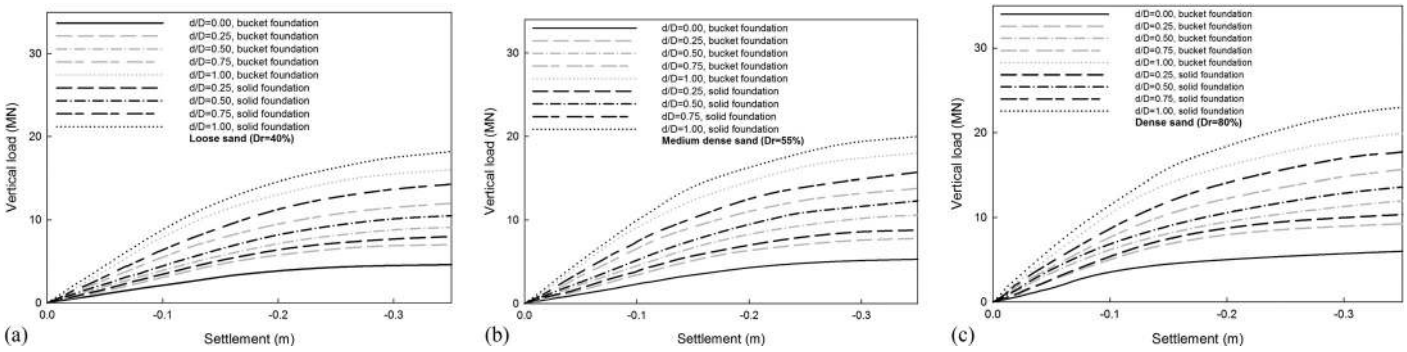

Fig. 14. Load-settlement response of suction bucket and equivalent solid foundations for (a) loose, (b) medium-dense, and (c) dense sand

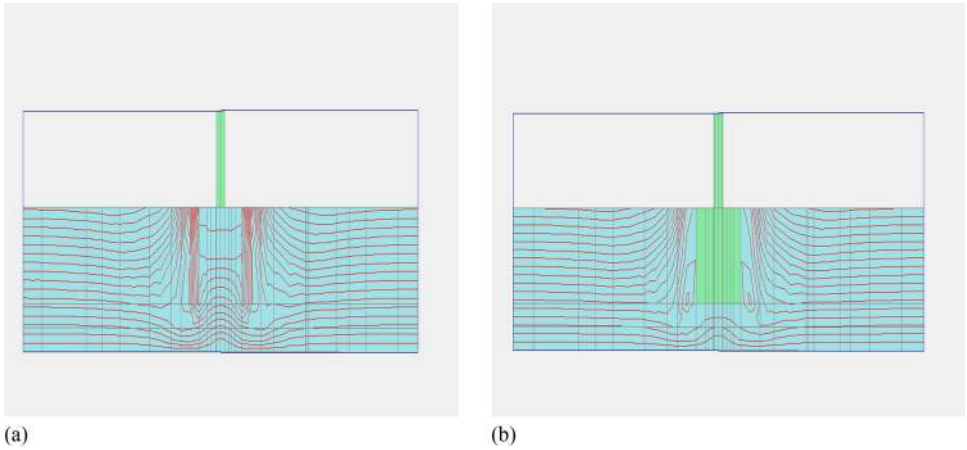

Fig. 15. Calculated failure mechanisms with d/D = 1: (a) FE bucket foundation; (b) embedded foundation

Downloaded from ascelibrary.org by Amin Barari on 09/30/16. Copyright ASCE. For personal use only; all rights reserved.

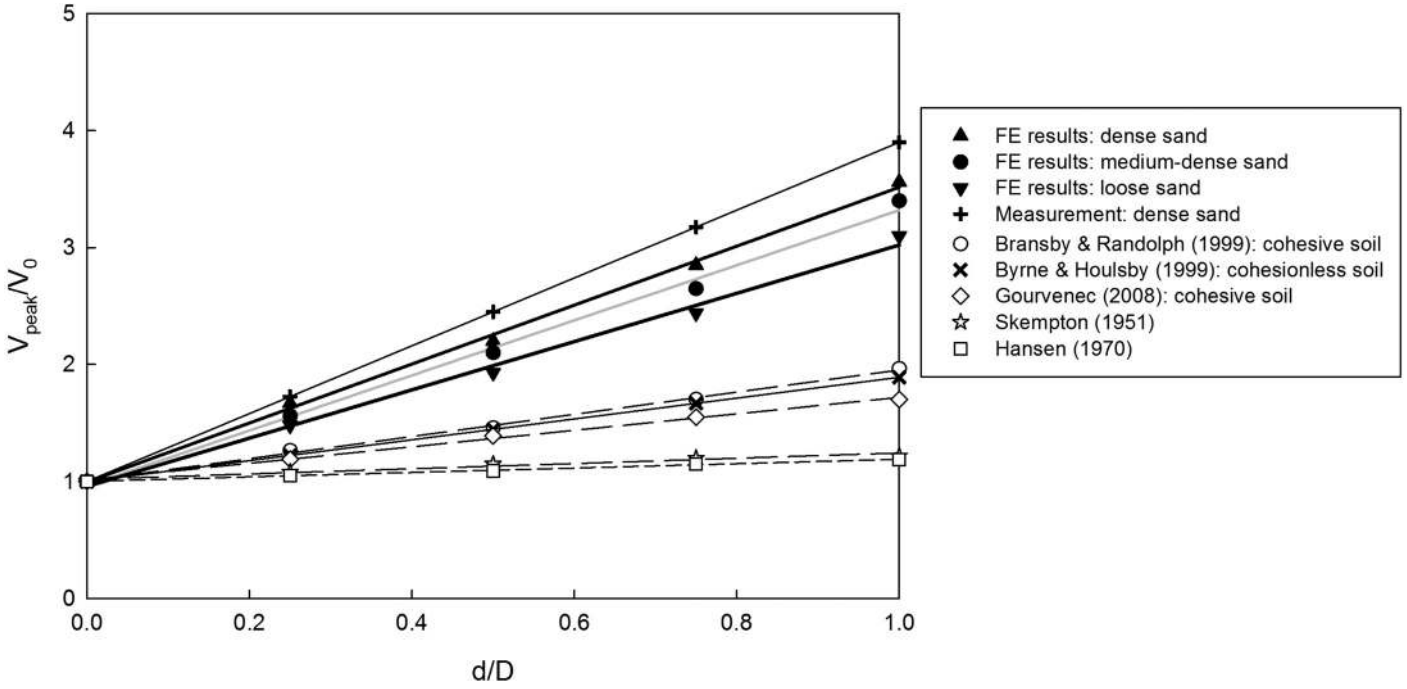

Fig. 16. Vertical bearing capacity factor as a function of embedment ratio

foundation and soil (Martin 2004; Barari and Ibsen 2012). This approach leads to underestimation of the FE solution and present measurements by over 37 and 40%, respectively, for the shallowest depth on the dense profile.

The conventional semiempirical depth factors (Skempton 1951; Meyerhof 1953; Brinch Hansen 1970) have suggested that depth factor (d_{cV}) may be approximated as a linear function of the normalized depth (d/D)

$$d_{cV} = 1 + n\frac{d}{D} \tag{10}$$

where n = fitting parameter. One of the aims of present study is to verify this approach.

The relationship between d_{cV} and d/D is almost linear, and an approximation depends on relative density. However, previous design recommendations for circular footings suggest that the factor n should lie in the range of 0.2–0.4, which significantly underpredicts the embedment effects observed with the data from FE analysis for suction caissons. FE analysis of a foundation with $d/D = 0.25$ in dense sand revealed that $d_c = 1.625$, which compares well with the loading test giving $d_c = 1.725$.

Also shown in Fig. 16 is the embedment factor against embedment ratio for the soil conditions with $D_r = 55$ and 80%, so almost linear relationships can be approximated by

$$\begin{aligned}(d_{cV_{ult}})_{\text{dense sand}} &= 1 + 2.5(d/D)\\ (d_{cV_{ult}})_{\text{medium-dense sand}} &= 1 + 2.2(d/D)\\ (d_{cV_{ult}})_{\text{loose sand}} &= 1 + 2(d/D)\end{aligned} \tag{11}$$

Conclusions

A series of FE calculations were carried out to investigate the vertical capacity of suction bucket and equivalent solid embedded foundations in cohesionless soil. In what follows, the results deduced from the analyses are compared to the results of model tests of caissons.

The studies can be successfully interpreted in the context of hardening plasticity theory by expressing size of yield locus as a function of vertical load and plastic vertical penetration.

As a part of this study, an investigation of the interaction between friction angle and total bearing capacity suggested that contribution of the deformations during the loading process is likely to be of significance in promoting a large scatter in the relationship between the vertical capacity and relative density. It was found that the proposed relationship using a reduced friction angle of 42° captured the measured capacities well and is very accurate, efficient, and convenient for stress levels under which the experiments were performed and for the sand tested. Comparison of the results from the new design concepts developed from the numerical analyses with the physical model revealed good agreement, validating them.

For the case of both foundation embedment and varying soil profiles (i.e., relative densities), the conventional approaches give an underestimate of d_{cV} owing to work hardening while capacity is mobilized.

The analyses also showed that the capacity of suction caissons could be less than expected with a larger disparity for the shallower embedment ratios if they were modeled as a solid foundation for uniform soil strength conditions. This observation may be attributed to the subtle changes in deformation mechanisms between foundations.

Alternative design concepts were finally presented for a range of complexities (for example, the effects of foundation shapes in 3D conditions, soil deformations in the vicinity of the foundation area, and a range of soil conditions). However, these issues are believed to be pertinent for many realistic foundation and soil conditions.

References

Andersen, K. H., et al. (2005). "Suction anchors for deepwater applications." *Proc., Int. Symp. on Frontiers in Offshore Geotechniques (ISFOG),* Keynote Lecture, CRC Press/Balkema, Rotterdam, Netherlands, 3–30.

Barari, A. (2012). "Characteristic behavior of bucket foundations." Ph.D. thesis, Aalborg Univ., Aalborg, Denmark.

Downloaded from ascelibrary.org by Amin Barari on 09/30/16. Copyright ASCE. For personal use only; all rights reserved.

Barari, A., and Ibsen, L. B. (2012). "Undrained response of bucket foundations to moment loading." *Appl. Ocean Res.*, 36, 12–21.
Barari, A., and Ibsen, L. B. (2014). "Vertical capacity of bucket foundations in undrained soil." *J. Civ. Eng. Manage.*, 20(3), 360–371.
Bhattacharya, S., Cox, J. A., Lombardi, D., and Wood, D. M. (2013). "Dynamics of offshore wind turbines supported on two foundations." *Proc. Inst. Civ. Eng. Geotech. Eng.*, 166(2), 159–169.
Bolton, M. D., and Lau, C. K. (1993). "Vertical bearing capacity factors for circular and strip footings on Mohr-Coulomb soil." *Can. Geotech. J.*, 30(6), 1024–1033.
Bransby, M. F., and Randolph, M. F. (1999). "The effect of embedment depth on the undrained response of skirted foundations to combined loading." *Soils Found.*, 39(4), 19–33.
Brinch Hansen, J. (1970). "A revised and extended formula for bearing capacity." *Danish Geotech. Inst. Bull.*, 28, 5–11.
Butterfield, R., and Gottardi, G. (1994). "A complete three-dimensional failure envelope for shallow footings on sand." *Géotechnique*, 44(1), 181–184.
Byrne, B. W., and Houlsby, G. T. (1999). "Drained behaviour of suction caisson foundations on very dense sand." *Offshore Technology Conf.*, Oxford Univ., Oxford, U.K., 10994.
Byrne, B. W., and Houlsby, G. T. (2001). "Observations of footing behaviour on loose carbonate sands." *Géotechnique*, 51(5), 463–466.
Byrne, B. W., Villalobos, F., Houlsby, G. T., and Martin, C. M. (2003). "Laboratory testing of shallow skirted foundations in sand." *Proc., BGA Int. Conf. on Foundations*, Thomas Telford, London, 161–173.
Cassidy, M. J. (2007). "Experimental observations of the combined loading behaviour of circular footings on loose silica sand." *Géotechnique*, 57(4), 397–401.
Danish Standards. (1998). "Norm for fundering (code of practice for foundation engineering)." *DS 415*, 4th Ed., Copenhagen, Denmark (in Danish).
Davis, E. H., and Booker, J. R. (1973). "The effect of increasing strength with depth on the bearing capacity of clays." *Géotechnique*, 23(4), 551–563.
EAU. (2004). "Empfehlungen des arbeitsausschusses 'ufereinfassungen' häfen und wasserstraßen EAU 2004." Ernst & Sohn, Berlin, Germany.
Feld, T. (2001). "Suction buckets, a new innovative foundation concept, applied to offshore wind turbines." Ph.D. thesis, Aalborg Univ., Aalborg, Denmark.
Gottardi, G., and Butterfield, R. (1993). "On the bearing capacity of surface footings on sand under general planar loads." *Soils Found.*, 33(3), 68–79.
Gottardi, G., and Butterfield, R. (1995). "The displacement of a model rigid surface footing on dense sand under general planar loading." *Soils Found.*, 35(3), 71–82.
Gottardi, G., Houlsby, G. T., and Butterfield, R. (1999). "Plastic response of circular footings on sand under general planar loading." *Géotechnique*, 49(4), 453–470.
Gourvenec, S. (2008). "Effect of embedment on the undrained capacity of shallow foundations under general loading." *Géotechnique*, 58(3), 177–185.
Guo, W. D., and Qin, H. Y. (2010). "Thrust and bending moment of rigid piles subjected to moving soil." *Can. Geotech. J.*, 47(2), 180–196.
Houlsby, G. T., and Byrne, B. W. (2005). "Design procedures for installation of suction caissons in sand." *Proc. Inst. Civ. Eng. Geotech. Eng.*, 158(3), 135–144.
Houlsby, G. T., Ibsen, L. B., and Byrne, B. W. (2005). "Suction caissons for wind turbines." *Int. Symp. on Frontiers in Offshore Geotechnics*, Taylor and Francis, London.
Houlsby, G. T., and Wroth, C. P. (1983). "Calculation of stresses on shallow penetrometers and footings." *Proc., IUTAMIIUGG Symp. on Seabed Mechanics*, Springer, Newcastle, U.K., 107–112.
Ibsen, L. B. (2008). "Implementation of a new foundation concept for offshore wind farms." *Int. Proc. 15th Nordic Geotechnical Meeting*, Norway, 19–33.
Ibsen, L. B., Barari, A., and Larsen, K. A. (2012). "Modified vertical bearing capacity for circular foundations in sand using reduced friction angle." *Ocean Eng.*, 47, 1–6.
Ibsen, L. B., Barari, A., and Larsen, K. A. (2014a). "Adaptive plasticity model for bucket foundations." *J. Eng. Mech.*, 10.1061/(ASCE)EM.1943-7889.0000633, 361–373.
Ibsen, L. B., Barari, A., and Larsen, K. A. (2015). "Effect of embedment on the plastic behavior of bucket foundations." *J. Waterway, Port, Coastal, Ocean Eng.*, 10.1061/(ASCE)WW.1943-5460.0000284, 06015005.
Ibsen, L. B., Borup, M., and Hedegaard, J. (1995). "*Data report 9501: Triaxial tests on baskarp sand no. 15*, Geotechnical Engineering Group, Aalborg Univ., Aalborg, Denmark.
Ibsen, L. B., Larsen, K. A., and Barari, A. (2014b). "Calibration of failure criteria for bucket foundations on drained sand under general loading." *J. Geotech. Geoenviron. Eng.*, 10.1061/(ASCE)GT.1943-5606.0000995, 04014033.
Ibsen L. B., Liingaard, M., and Nielsen, S. A. (2005). "Bucket foundation, a status." *Conf. Proc., Copenhagen Offshore Wind*, IEC, Copenhagen, Denmark.
Jeong, S., Lee, J., and Lee, C. (2004). "Slip effect at the pile-soil interface on dragload." *Comput. Geotech.*, 31(2), 115–126.
Larsen, K. A., Ibsen, L. B., and Barari, A. (2013). "Modified expression for the failure criterion of Bucket foundations subjected to combined loading." *Can. Geotech. J.*, 50(12), 1250–1259.
LeBlanc, C., Houlsby, G. T., and Byrne, B. W. (2010). "Response of stiff piles in sand to long-term cyclic lateral loading." *Géotechnique*, 60(2), 79–90.
Lundgren, H., and Mortensen, K. (1953). "Determination by the theory of plasticity of the bearing capacity of continuous footings on sand." *Proc., Third Int. Conf. Soil. Mech*, Zurich, Switzerland, 1.
Mansur, C. I., and Kaufman, J. M. (1956). "Pile tests, low-sill structure, Old River, Louisiana." *J. Soil Mech. Found. Div.*, 82(SM5), 1–33.
Martin, C. M. (1994). "Physical and numerical modelling of offshore foundations under combined loads." D.Phil. thesis, Univ. of Oxford, Oxford, U.K.
Martin, C. M. (2004). "User guide for ABC-Analysis of Bearing Capacity." Version 1, *OUEL Rep. No.226/03*, Dept. of Engineering Science, Univ. of Oxford, Oxford, U.K.
Meyerhof, G. G. (1953). "The bearing capacity of footing under eccentric and inclined loads." *Proc., 3rd Int. Conf. on SMFE*, Zurich, 440–445.
Nova, R., and Montrasio, L. (1991). "Settlements of shallow foundations on sand." *Géotechniqué*, 41(2), 243–256.
Ohde, J. (1939). "Zur Theorie der Druckverteilung im Baugrund." *Bauingenieur*, 20, 451–459.
PLAXIS 3D [Computer software]. Plaxis bv, Delft, Netherlands.
Popescu, R., and Prevost, J. H. (1993). "Centrifuge validation of a numerical model for dynamic soil liquefaction." *Soil Dyn. Earthquake Eng.*, 12, 73–90.
Prandtl, L. (1920). "Uber die Harte plastischer Korper." *Nachr. D. Ges. D. Wiss. Gottingen, Math. Phys. Klesse*, 74–85 (in German).
Roscoe, K. H., and Schofield, A. N. (1956). "The stability of short pier foundations in sand." *Br. Weld. J.*, 3(8), 343–354.
Sieffert, J. G., and Bay-Gress, C. (2000). "Comparison of European bearing capacity calculation methods for shallow foundations." *Proc. Inst. Civ. Eng. Geotech. Eng.*, 143(2), 65–74.
Skempton, A. W. (1951). "The bearing capacity of clays." *Proc., Building Research Congress*, ICE, London, Vol. 1, 180–189.
Tahmasebi poor, A., Barari, A., Behnia, M., and Najafi, T. (2015). "Determination of the ultimate limit states of shallow foundations using gene expression programming (GEP) approach." *Soils Found.*, 55(3), 650–659.
Tani, K., and Craig, W. H. (1995). "Bearing capacity of circular foundations on soft clay of strength increasing with depth." *Soils Found.*, 35(4), 21–35.
Terzaghi, K. (1943). *Theoretical soil mechanics*, Wiley, New York.
Tjelta, T. I. (1995). "Geotechnical experience from the installation of the Europipe jacket with bucket foundations." *Proc., Offshore Technology Conf.*, Houston, TX, Paper No. 7795.
Villabolos, F. A., Byrne, B. W., and Houlsby, G. T. (2005). "Moment loading of caissons installed in saturated sand." *Int. Symp. on Frontiers in Offshore Geotechnics*, Perth, Western Australia.

Downloaded from ascelibrary.org by Amin Barari on 09/30/16. Copyright ASCE. For personal use only; all rights reserved.